Synthetic efforts and computational modeling towards nitrogen-containing curcumin-related compounds.

Student Author: Trudeau, C. R.

Faculty Sponsor: Stepanova V. A.

ABSTRACT

Curcumin is one of the compounds found in turmeric. Due to its high conjugation, curcumin is a bright yellow pigment and is found in applications such as food coloring and additives. Curcumin has demonstrated a broad range of medicinal applications. However, curcumin suffers from very poor water solubility which hinders its pharmacological use. In addition to the extraction from plants, curcumin can be synthesized through a Claisen-Schmidt condensation reaction between vanillin serving as an aldehyde component and acetylacetone in place of a ketone. Our group previously reported the solvent-free procedure towards synthesis of curcumin and its close analogous, curcuminoids. In this project we focused our efforts on expanding our methodology to obtain curcumin analogs that contain nitrogen. The objectives of the study were to test the methodology and to isolate a curcuminoid with potentially enhanced water solubility. This study applied two different approaches towards the research goals: theoretical calculations and synthesis. Computational analysis was used to determine if the anticipated products are thermodynamically favorable, and if there is a potential thermodynamic preference between anticipated products. Additionally, the synthetic efforts focused on isolating nitrogen-containing curcumin analogs. The theoretical data demonstrates that all possible products have positive Gibbs free energy values. This supports the hypothesis that the studied processes are not spontaneous and potentially governed by kinetic control. The experimental data and spectroscopic observations support formation of the desired product. Further investigations will be needed to clearly elucidate the extent of a thermodynamic or a kinetic control occurring in the studied processes.

INTRODUCTION

Curcumin is a naturally occurring molecule found in the plant *Curcuma longa* and most notably found in the spice, turmeric [3]. In recent years, curcumin and analogous compounds known as curcuminoids have found numerous medicinal applications. Curcumin has been gaining attention in the medicinal community due to its' discovered anti-oxidizing [1], [3], [4], anti-inflammatory [2], anti-cancer [5], anti-aging [6], [7], and neuroprotective effects [8], all of which have been supported through laboratory and clinical studies. Despite its recognized biological activity, curcumin is a poor drug candidate due to several limitations. One of the most severe limitations is the poor water solubility of curcumin, leading to poor bioavailability [8]. Therefore, we are particularly interested in curcumin's water solubility. Additionally, the low concentration of curcumin in water solutions decomposes in vivo; providing another limitation of curcumin [8]. Since water is the main solvent in all cells, this severely hinders the consumption of the active ingredients of curcumin and severely limits the medicinal applications of curcumin [9]. To increase water solubility and stability of curcumin, unnatural analogs of curcumin known as curcuminoids have been synthesized and demonstrated enhanced solubilities and overall biological effects [5].

Even though most studies on the bioactivity of curcumin commonly use the one isolated from natural source, curcumin can also be synthesized. Curcumin can be obtained by an aldol condensation reaction with vanillin as an aldehyde component and acetylacetone as a ketone. The resulting structure (Scheme 1) consists of two arm pieces from the aldehyde shown in blue and one core linker from the ketone shown in red. The new bond that combines those pieces is indicated in black. Due to the presence of a highly conjugated system curcumin appears as a bright yellow powder or yellow solution under neutral or slightly acidic pH. The color of curcumin changes to blood red under basic pH [5].

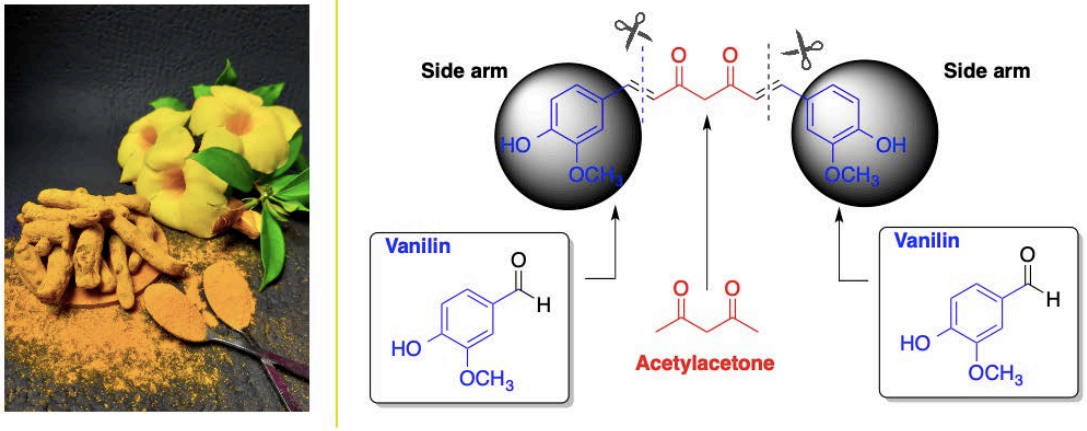

Scheme 1. General structure build of curcumin. Photo by Tamanna Rumee on Unsplash.

Studies show that the replacement of the symmetric flexible acetyl acetone linker (Scheme 1, shown in red) found in natural curcumin with an asymmetric rigid 3-acettylacetone linker (Scheme 2, shown in red) enhances the stability of resulting compounds in vivo [10]. The solubility greatly depends on the functional groups present on the side arms aromatic rings (Scheme 1, shown in blue). In our proposal, we suggest combining two synthetic modification approaches by introducing nitrogen atoms in the side arm fragments and an asymmetric linker to replace core fragment of curcumin to potentially generate a new class of curcuminoid therapeutics (Scheme 2).

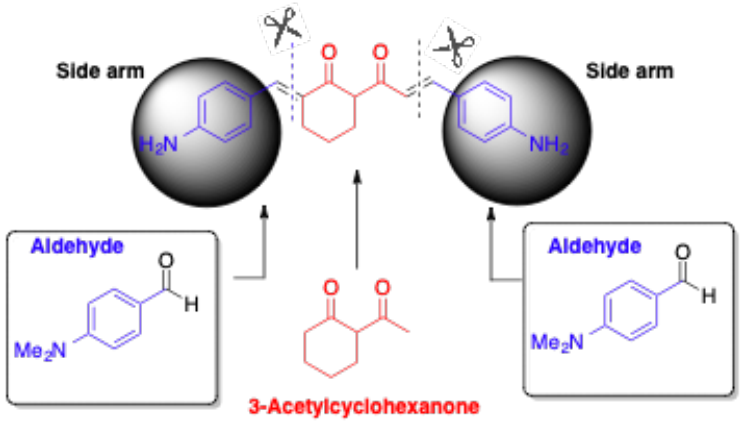

Scheme 2: Proposed new class of curcuminoids with a potential improved water solubility and overall stability.

The reasoning behind our approach is in part due to the known ability of nitrogen to act as a hydrogen bond acceptor. As seen in curcumin, without the nitrogen in the ring system to participate in the hydrogen bonding network, there is a very low water solubility. This is because carbon cannot participate in hydrogen bonds like nitrogen and is more hydrophobic. Because of the high affinity ("love") of nitrogen to water this modification will enhance water solubility of resulting compounds. As a result, obtained nitrogen containing curcuminoids can have potential to integrate more readily into the hydrogen bonding network of water and be dissolved more easily (Scheme 3).

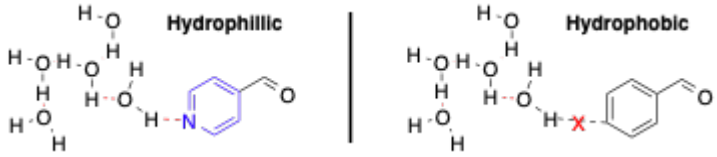

Scheme 3: hydrophilic and hydrophobic interactions with water

The restriction of geometry posed by the asymmetric linker can increase stability of products (Scheme 4). The flexibility of acetyl acetone bridge in original curcumin affects its ability to bind proteins [10]. Substitution of flexible bridge with a cyclic one removes possibility of flex or rotation. Our hypothesis is that since these modification does not affect electron count of the molecule the biological potential will remain. Due to the dual focus of our synthetic efforts this research will lead to isolation of new curcuminoids with altered structure, selected specific chemical properties, and potentially enhanced solubilities that have not been attained before (Scheme 4).

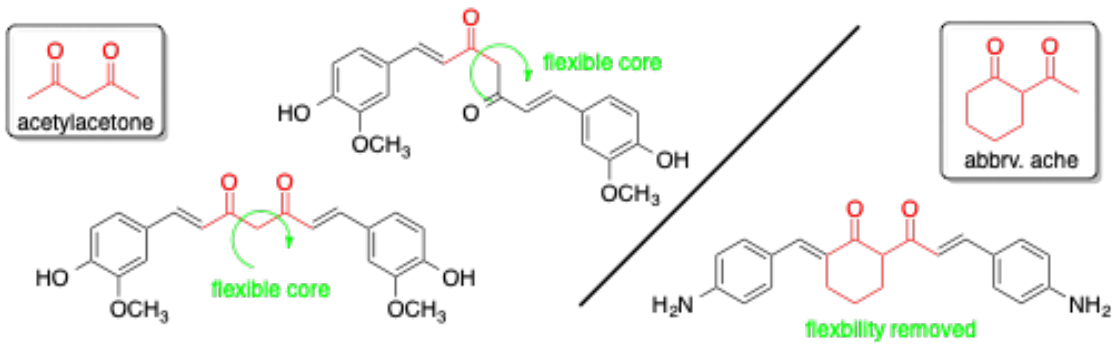

Scheme 4: Difference in flexibility of acetyl acetone bridge versus ache bridge.

METHODS

We approached this research question from two perspectives: synthetic and computational. Our synthetic efforts were complimented by computational modeling of starting materials and possible products. All structures were modeled at the HF/3-21+G*/(PCM:$CHCl_3$) level of theory using the computational chemistry suite GAMESS [12] (5 Dec 2014 R1). All structures were verified as true minima as indicated by the absence of any imaginary vibrational frequencies. Structures were pre-optimized using Avogadro and visualizations were produced using wxMacMolPlt. Wet experiments were aimed on isolation of compounds using microwave solvent-free synthesis approach that was previously used in our group [16].

Synthesis. Previously our group developed solvent-free methods towards curcuminoid using conventional heat and side arm modifications [16, Scheme 5a], and microwave energy to obtain asymmetric curcuminoids using a cyclic core piece (WiSys T210036, Scheme 5b). In this research, we combined the microwave energy solvent-free synthetic protocol with the isolation protocol developed for the conventional heat solvent-free protocol used by our group towards syntheses of nitrogen-containing curcuminoids.

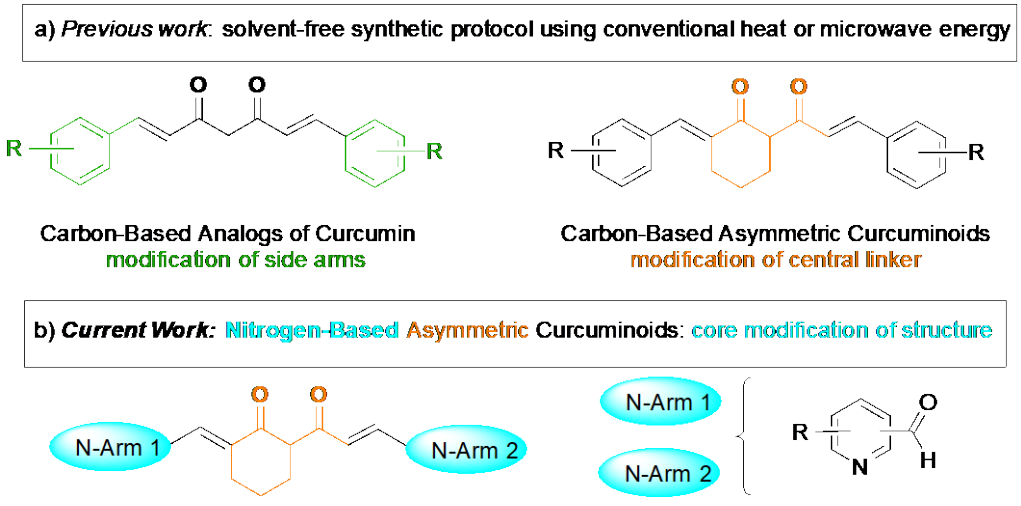

Scheme 5: Perspective on the research innovation of this project.

Computational. The mechanism of the reaction was previously proposed by our group [16]. Formation of the final product, hereafter referred to as di-addition product **3** precedes in the mechanism by formation of two mono-addition products compounds **1** and **2** (Table 1, columns 2 and 3). Due to the asymmetric diketone central linker structural piece, each of the proposed products can theoretically exist as a tautomer with two possible enol forms labeled as **a** and **b**, where the position of double bond and OH-group interchange. To summarize there are six intermediates to be considered (Table 1, columns 2 and 3). All of the possible compounds were analyzed using computational methods to determine the thermodynamic preference for the first addition and formation of the mono-product as well as thermodynamic preference for the particular form of the compound, such as diketo or enol **a** or **b**.

Table 1. Summary of three products and their respective tautomers. In blue and green are two potential mono-addition products, and in red is the di-product. All structures were analyzed computationally.

Product	**Mono addition products**		**Di-addition product**
Form	Category 1	Category 2	
Diketone	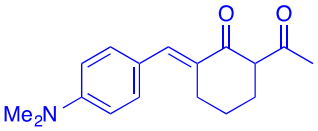	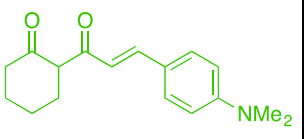	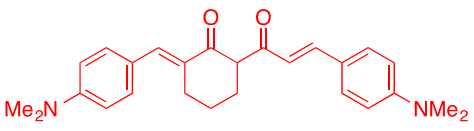
Enol a	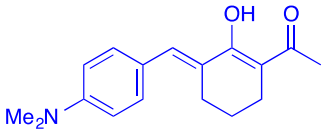	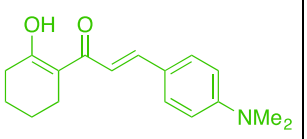	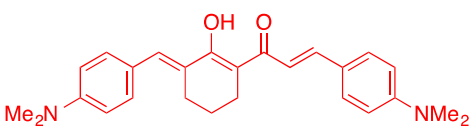
Enol b	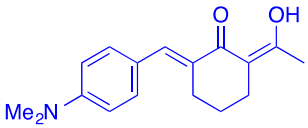	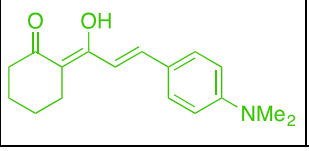	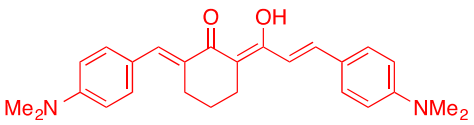

EXPERIMENTAL

All chemicals and solvents were purchased from Sigma-Aldrich and used without further purification. Spectroscopic data were collected using 400 MHz Bruker Avance spectrometer and Perkin Elmer FT-IR instrument with ATR attachment and a diamond crystal. The chemical shifts (δ) are reported in parts per million relative to the residual deuterated solvent signal, and coupling constants (J) are given in Hertz. Melting points were collected using DigiMelt and are uncorrected. Microwave experiments were performed using Biotage® Initiator+ equipped with a Robot 8 accessory and using original Biotage® single use 5 mL vials. Elemental analyses were acquired using external services (Atlantic Microlabs). High-resolution mass spectrometry data (HRMS) were acquired in collaboration with Dr. Kubatova's research group at the University of North Dakota (UND).

General synthesis of the target curcuminoid, 2-[(*E*)-3-(4-*N*,*N*-dimethylphenyl)acryloyl]-6-[1-(4-chlorophenyl)meth-(*E*)-ylidene]-cyclohexanone

To a vial, boric anhydride (0.1253 mg, 1.8 mmol) and 2-acetylacetone (0.325 mL, 2.5 mmol) was added along with a stir bar. To the same vial tri(n-butyl)borate (2.698 mL,10 mmol) was added. The reaction was stirred for several minutes which followed by addition of *N*,*N*-dimethylbenzaldehyde (0.7609 mg, 5.1 mmol). At this point, the reaction was capped and wrapped in foil to avoid light exposure. After addition of the n-butylamine (0.100 mL, 1 mmol) using a syringe through the septa the foil was removed and reaction mixture was placed in the Robot 8 of microwave reactor. The reaction was conducted at elevated temperature at a stir rate of 900 rpm, ensuring the cooling feature is on to minimize temperature fluctuation. After heating was completed ethanol (3.0 mL) was added to the mixture through the septum and digestion was completed at 95°C for 22:32 minutes with a stir rate of 900 rpm and cooling feature on.

General isolation of the target curcuminoid, 2-[(*E*)-3-(4-*N*,*N*-dimethylphenyl)acryloyl]-6-[1-(4-chlorophenyl)meth-(*E*)-ylidene]-cyclohexanone

After removing the mixture from the reactor, and upon cooling, the product precipitated. The product was isolated using vacuum filtration and rinsed with cold ethanol. After drying in vacuum oven for 5 hrs at 65 °C the curcuminoid

was isolated as a blue solid. ^{1}H NMR (400 MHz, $CDCl_3$): 1.79 (m, 2H, -CH_2-), 2.64 (m, 2H, -CH_2-), 2.78 (t, *J* = 6.9 Hz, 2H, -CH_2-), 3.01 (s, 6H, -NMe_2), 3.03 (s, 6H, -NMe_2), 5.30 (s, 0.30H, -C(O)-CH-C(O)-), 6.68 (d, *J* =8.0 Hz, 2H, CH), 6.71 (d, *J* =8.0 Hz, 2H, CH), 6.90 (d, *J* = 15.4 Hz, 1H, -CH=CH-C(O)-), 7.39 (d, *J* = 8.9 Hz, 2H, CH), 7.49 (d, *J* = 8.9 Hz, 2H, CH), 7.65 (s, 1H, -CH=C-C(O)-), 7.71 (d, *J* = 15.4 Hz, 1H, -CH=CH-C(O)-), 17.58 (s, 0,84H, -C(O)-C=C(OH)-). Calc. for $C_{26}H_{30}N_2O_2$: C, 77.58; H, 7.51; N, 6.96. Found: C, 77.69; H, 6.90; N, 6.39. HRMS calc. for $C_{26}H_{31}N_2O_2^+$: 403.2380, found: 403.2461.

Optimization of reaction conditions for the target curcuminoid, 2-[(*E*)-3-(4-*N*,*N*-dimethylphenyl)acryloyl]-6-[1-(4-chlorophenyl)meth-(*E*)-ylidene]-cyclohexanone

The optimal conditions for the synthesis were found to be at 85°C for 11:15 minutes. Under these conditions the product was isolated in 74.1% yield (0.7700 g). Doubling of temperature decreased the yield of the product to 42.6% yield and doubling of time while maintaining reaction at 85°C decreased product yield to 32.4%.

RESULTS AND DISCUSSION

For relative comparison of reaction mixtures isolated during the optimization study of reaction conditions we superimposed all the ^{1}H NMR spectra using Bruker Topspin software (Figure 1). The reaction product isolated from optimal experimental conditions of 85°C and ~11 minutes reaction time is shown in green. The product isolated from double time experiment is shown in red and the one from double temperature experiment is in blue. For convenience the structures of product and corresponding aldehyde are shown on the spectra. In addition, the signals of interest are highlighted in the colors to facilitate the discussion.

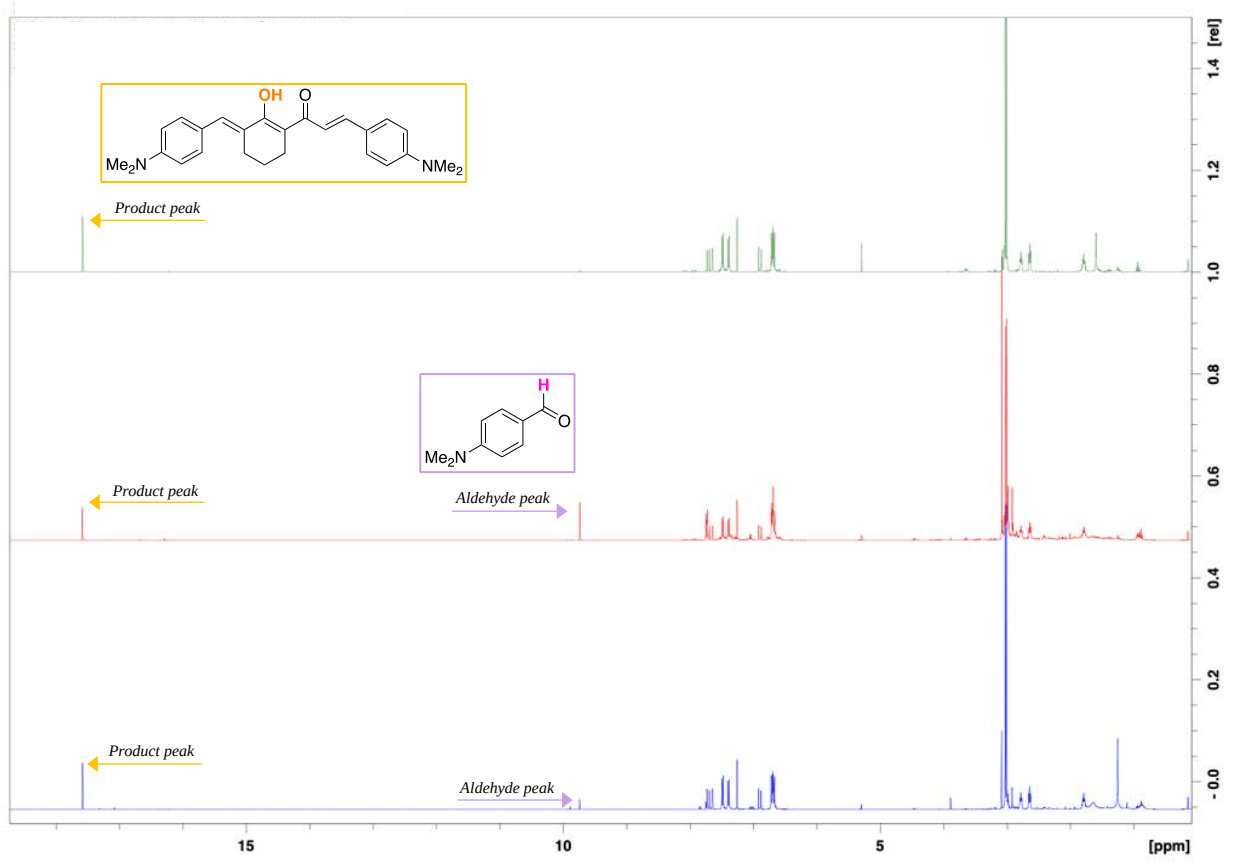

Figure 1: Side-by-side comparison of ^{1}H NMR for products isolated in optimization study.

The characteristic peak of the product is an enol peak appears in far downfield region (chemical shift δ ~18 ppm) and is indicative of the formation of connection between the 2-acetylcyclohexanone linker (ACHE) and the aldehyde. The product peak (Figure 1) was observed for all conditions as a sharp singlet. The remaining starting aldehyde can be easily identified by a peak near an aromatic region (chemical shift δ ~ 10 ppm). The most amount of aldehyde was observed for the double time experiment, however, elevation of temperature created additional unidentified impurities with signals in that area. The comparison of reaction mixtures using infrared (IR) spectrometry and thin-layer chromatography (TLC) was also undertaken. The overlap of IR spectra for all three mixtures showed identical profile. The separation of spotted reaction mixtures and aldehyde reference indicates also nearly identical distribution of components (Figure 2).

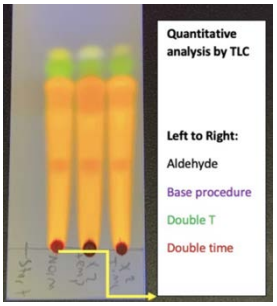

Figure 2: TLC data (hexane-acetone 2:1).

The impact of microwave assistance was evaluated using a control synthesis experiment. The reaction mixture was prepared using general synthesis outlined above with exceptions of temperature and time. After carrying out stirring for five days the mixture was subjected to an ethanol digest at 95°C for 22:32 minutes yielding a dark blue precipitate in the reaction vial. Typical crystallization with ethanol yielded no additional product. The comparison of isolated fractions was undertaken using ^{1}H NMR spectroscopy and the summary is shown on Figure 3.

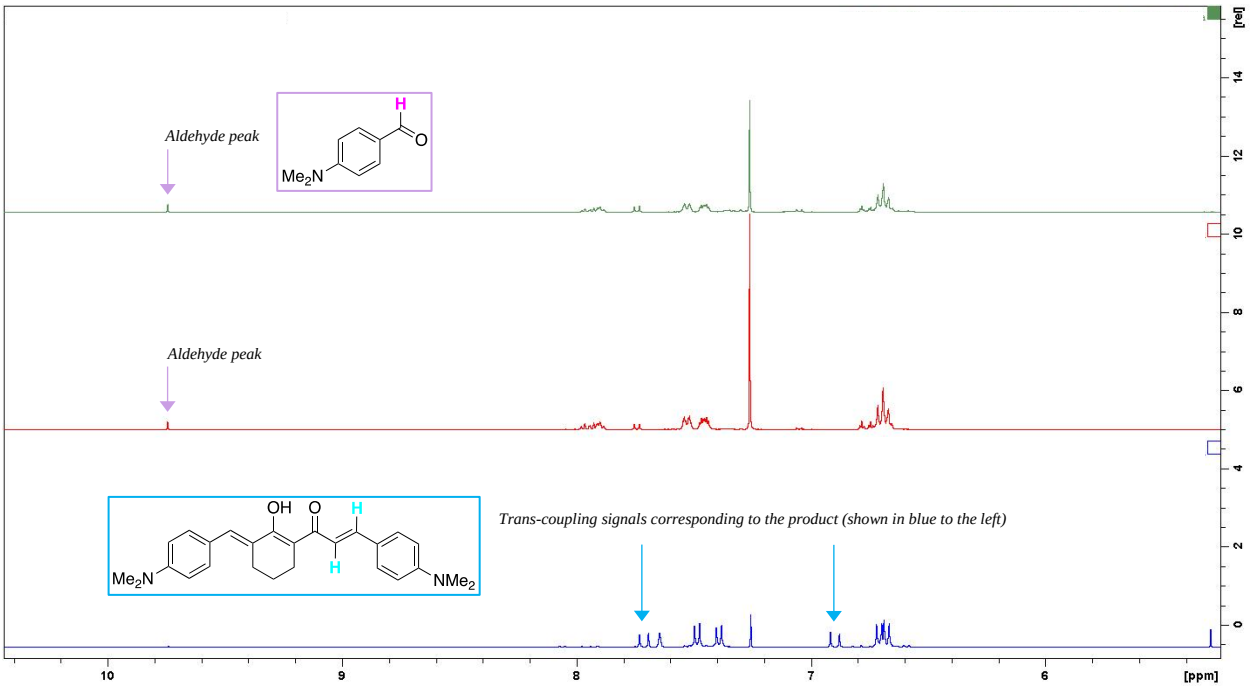

Figure 3: The comparison of a control experiment without MW is shown in blue (precipitate) and green (filtrate). Previous extended time experiment with MW assistance is shown in red.

The data clearly illustrate that product formation occurs under room temperature at prolonged times. The trans-coupling hydrogen signals undoubtfully indicate presence of the product (Figure 3). However, the absence of an aldehyde signal in the isolated precipitate cannot be acquitted to the complete consumption of an aldehyde during the reaction as it clearly appears in the filtrate. In addition, the isolated yield of the product (73%) was on par with the one obtained for the microwave experiments under optimized conditions. The main message of the control experiment, therefore, is an indirect indication that formation of product does not require substantial heating or, perhaps, the product itself is sensitive to heating beyond certain temperatures. Lack of previously reported literature data on preparation of the target curcuminoid makes it complicated to compare our microwave experiments to a conventional synthesis and further investigation will be required to elucidate temperature effect on the desired product formation and the product yield.

In addition to the temperature effect, we initiated an investigation of the effect of light on the starting aldehyde. The manufacturer of the starting material lists light sensitivity as an issue and recommends handling of this compound without proximity to a light source. To the best of our knowledge there was no reports on the impact of the light on the composition of the aldehyde. We conducted a series of ^{1}H NMR experiments monitoring the exposure of the *N*,*N*-dimethylbenzaldehyde, the starting aldehyde, to a short wave UV light. A summary of the experimental data is provided in Figure 4.

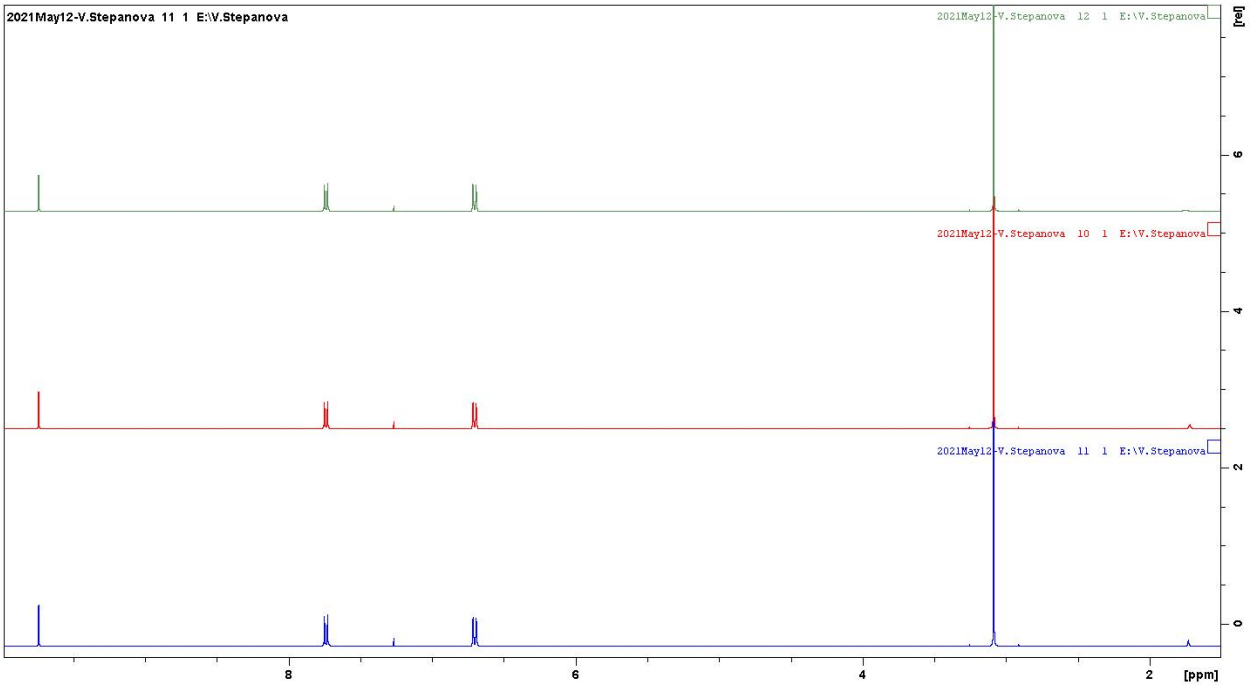

Figure 4: ^{1}H NMR spectral comparison of the changed in the starting aldehyde solution under UV exposure. Shown in red prior to exposure, in blue after 15 minutes, and in green after 40 minutes of continuous exposure.

The ^{1}H NMR data demonstrate virtually no changes to the composition of the solution (Figure 4). The preparation of sample was conducted in a standard manner by weighing ~20 mg of an aldehyde in the dark room and dissolving it in the ~0.5 mL of deuterated chloroform ($CDCl_3$). The typical ~CH=O aldehyde peak observed at high downfield range (δ ~10 ppm) did not disappear. The same was observed for the aromatic region which is typically characterized by a set of two doublets of equal integration. At last, the corresponding methyl group signal in the aliphatic range also did not disappear and was not altered in its appearance or integration. This experimental data is somewhat surprising as the visual changes of color were observed for the solution upon exposure to UV light (Figure 5). At the time of the sample, it appears as a clear and colorless solution which gradually acquires green tint to it within the first hour of exposure (Figure 5a). The continuous and prolonged UV exposure intensifies and changes color of the sample to bright yellow. However, we did not find any evidence of substantial changes on the molecular level for samples with drastic color appearance using ^{1}H NMR spectrometry.

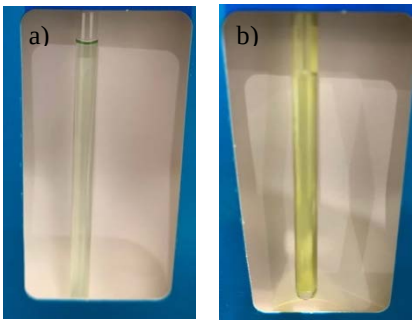

Figure 5: Visual changes of an NMR sample after a) 0.5 and b) 4 hrs.

Our synthetic efforts were matched up with computational investigation of the stepwise formation of the product. It is obvious that the attachment of both equivalents of an aldehyde must be sequential (for details see Table 1) however, which point of attachment is preferential is not straightforward. This matter is further complicated by the possibility of the coexistence of tautomers of the desired compound as those compounds are isomeric.

We calculated relative free energies (G, kJ/mol) of three possible forms of di-addition products one in the keto form, and two in the enol form (Figure 6). The keto form is characterized with the lowest value of free energy. This

is most likely due to the possibility of flexing as indicated by the 3D image. The two aromatic rings are clearly not coplanar, and the molecule has adapted a bent geometry overall. Both of enol tautomers exist in a substantially more rigid arrangement which is forced by the continuous conjugation due to positioning of the double bond on the cyclohexane ring at the diketone functionality. Interestingly, placement of the double bond outside of the ring substantially increases the stability of the molecule resulting in the lower G value when compared to the isomer with the double bond located at the cyclohexane ring.

All isomeric structures were modeled in the solvent phase. We chose chloroform to achieve the closest match to the conditions of ^{1}H NMR experiments. We observed a small difference between enol and keto forms of the product. At less than 2 kcal/mol difference it is not surprising that an enolic product appears to be the dominant form found in solution (Figure 3). The keto being of lower predicted energy likely is somewhat more indicative of potential shortcomings of this particular calculation method rather than any false spectral interpretation. It is somewhat more surprising that our theoretical modeling identified the substantial energy difference between the two enolic forms.

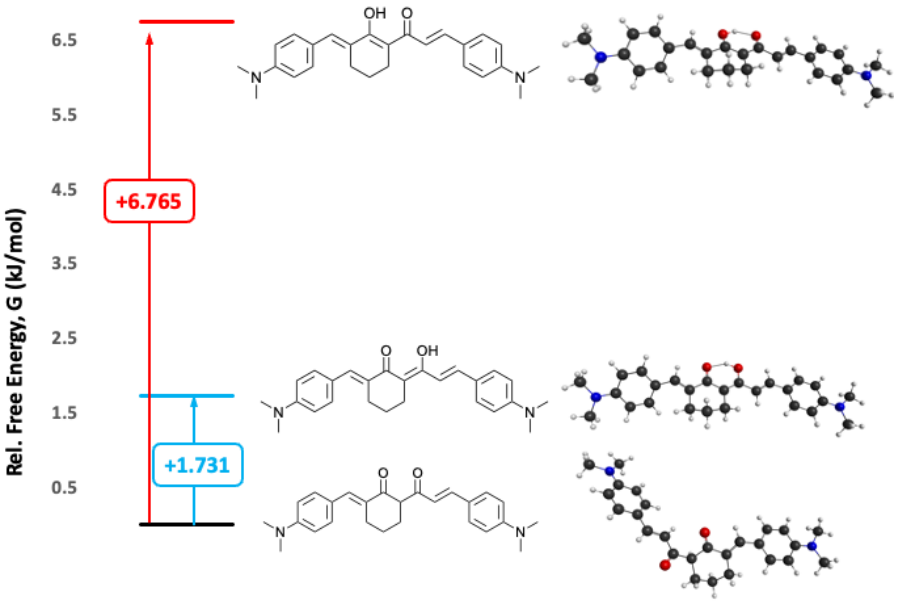

Figure 6: Relative free energies (G) of all tautomers of the disubstitued product.

2-Acetylcyclohexanone (ache), served as a central linker, as an analogue of acetylacetone ("acac") can undergo the same keto-enol tautomerization. Unlike acac, ache has an added complication of inequivalent enolic forms arising from the asymmetry of the molecule. It is well known that the enolic form of acac is favored in non-polar, non-H bonding solvents like chloroform. Given our above results (Figure 6) indicating preference for keto form over the two enolic forms we investigated if this was a result of the substitutions or was more intrinsic to this particular linker system. Again, we observe a relatively small difference (though larger now at nearly 3 kcal/mol) between the most favorable keto form and the enolic ache form in which the oxygen-bound hydrogen atom is more directly associated with the sidearm oxygen rather than the ring-attached oxygen.

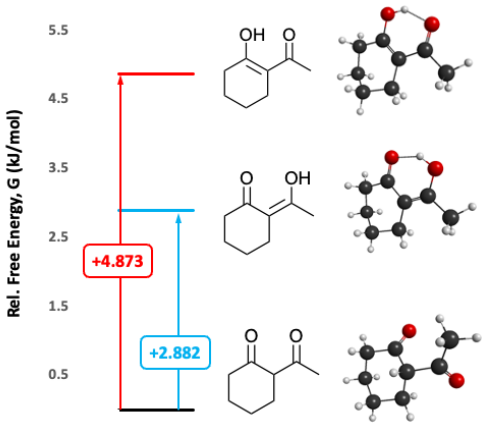

Figure 7: Relative free energies (G) of all tautomers of 2-acetylcyclohexanone.

Analysis of the mono-substituted products was undertaken to 1) aid in spectral interpretation of incomplete reaction mixtures and 2) to attempt to identify the preferred first addition site and thus begin mechanistic elucidation. In modeling all possible monoaddition products (two structural isomers, each with three tautomeric forms), we found the keto form of the ring-side attachment site (as opposed to attachment at the sidearm) to be most favorable. The substantial energy difference between the two lowest energy forms within each set (~4.4 kcal/mol) is quite large, indicating a clear thermodynamic preference for the single form.

When comparing the monoaddition sites as their own subset, the ring-side attachment set displayed a reversal in the relative energies of the enolic forms. Formal attachment of the enolic hydrogen to the ring-based oxygen allows extension of the conjugated system through the ring, whereas attachment at the sidearm oxygen causes an interruption in this conjugation. When comparing the sidearm attachment set, the relative favorability of the two enolic forms

aligns with the conventions observed for the unreacted linker as well as the diaddition product. Presumably, this is following the same pattern of thermodynamic selection for the structural form that maintains the longest, most extensive conjugated system.

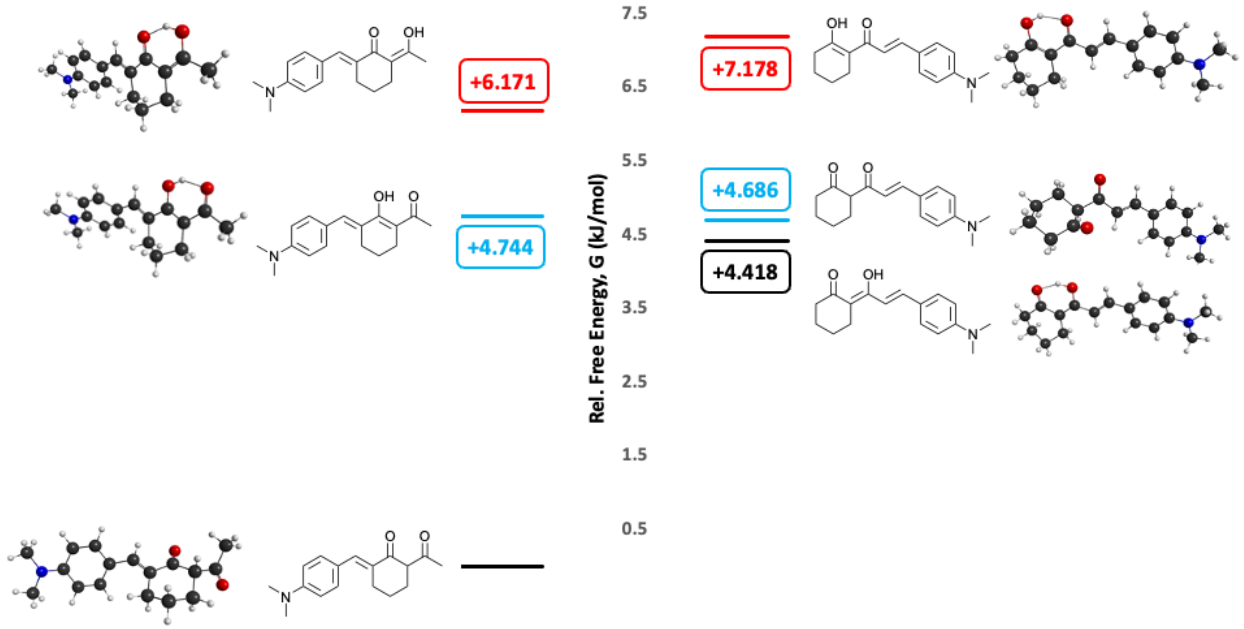

Figure 8: Relative free energies (G) of monosubstituted products.

CONCLUSION

Our investigation on synthesis of 2-[(*E*)-3-(4-*N*,*N*-dimethylphenyl)acryloyl]-6-[1-(4-chlorophenyl)meth-(*E*)-ylidene]-cyclohexanone using a combination of synthetic and computational approach provided the desired compound in a moderate to good yield. The optimization study indicated that high temperature is not recommended for the synthesis and results in a decreased product yield. The reasoning behind the effect is not fully understood and will require further investigation. Our computational efforts illustrate preference for the formation of mono-product on the acetyl group as the first step of the mechanism. In addition, we calculated free energies for each of the potential subsequent products in both keto and enol form. The theoretical data also indicate the energy preference for the existence of product in the keto form rather than either of the two possible enol arrangements.

ACKNOWLEDGEMENT

The authors acknowledge the Minnesota Supercomputing Institute (MSI) at the University of Minnesota for providing resources that contributed to the research results reported within this paper. URL: http://www.msi.umn.edu. The authors acknowledge the Department of Chemistry at Winona State University for the access to their JEOL ECX-300 NMR spectrometer to collect research results reported within this paper. The instrument was funded by NSF Award #DUE-0126470 in 2001. The authors acknowledge the Department of Chemistry at UW–La Crosse for the access to Bruker Avance III 400 NMR spectrometer to collect research results reported within this paper. The instrument was funded by NSF Award #CHE-0923388 in 2009.The authors acknowledge UW–La Crosse Undergraduate Research and Creativity Office for the financial support provided to undergraduate research students author ($2,000 URC grant Fall 2020 and $1,927 URC grant Spring 2021).

REFERENCES

[1] Sahebkar A., Serbanc M.C., Ursoniuc S., Banach M. (2015). Effect of curcuminoids on oxidative stress: A systematic review and meta-analysis of randomized controlled trials. *J. Funct. Foods*. **18**, 898–909.

[2] Panahi, Y., Hosseini, M. S., Khalili, N., Naimi, E., Simental-Mendía, L. E., Majeed, M., & Sahebkar, A. (2016). Effects of curcumin on serum cytokine concentrations in subjects with metabolic syndrome: A post-hoc analysis of a randomized controlled trial. *Biomed. Pharmacother.* **82**, 578-582.

[3] Lao, C. D., Ruffin, M. T., Normolle, D., Heath, D. D., Murray, S. I., Bailey, J. M., & Brenner, D. E. (2006). Dose escalation of a curcuminoid formulation. *BMC Complem. Altern. M.* **6**, 1-4.

[4] Jurenka, J. S. (2009). Anti-inflammatory properties of curcumin, a major constituent of Curcuma longa: a review of preclinical and clinical research. *Altern. Med. Rev.* **14**, 141-53.

[5] Goel, A., Kunnumakkara, A. B., & Aggarwal, B. B. (2008). Curcumin as "Curcumin": from kitchen to clinic. *Biochem. Pharmacol.* **75**, 787-809.

[6] Lima, C. F., Pereira-Wilson, C., & Rattan, S. I. (2011). Curcumin induces heme oxygenase-1 in normal human skin fibroblasts through redox signaling: Relevance for anti-aging intervention. *Mol. Nutr. Food Res.* **55**, 430-442.

[7] Shailaja, M., Gowda, K. D., Vishakh, K., & Kumari, N. S. (2017). Anti-aging role of curcumin by modulating the inflammatory markers in albino wistar rats. *J. Natl. Med. Assoc.* **109**, 9-13.

[8] Modasiya, M. K., & Patel, V. M. (2012). Studies on solubility of curcumin. *Int. J. Pharm. Life Sci*. **3**, 1490-1497.

[9] Thiyagarajan, M., & Sharma, S. S. (2004). Neuroprotective effect of curcumin in middle cerebral artery occlusion induced focal cerebral ischemia in rats. *Life Sci*. **74**, 969-985.

[10] Tham, C. L.; Harith, H. H.; Lam, K. W.; Chong, Y. J.; Cheema, M. S.; Sulaiman, M. R.; Lajis, N. H.; Sulaiman, M. R.; Lajis, N. H.; Israf, D. A. (2015). The synthetic curcuminoid NHMC restores endotoxin-stimulated HUVEC dysfunction: Specific disruption on enzymatic activity of p38 MAPK. *Eur. J. Pharm.* 1–11.

[11] Binkley, J. S.; Pople, J. A.; Hehre, W. J. (1980). Self-consistent molecular orbital methods. 21. Small split-valence basis sets for first-row elements. *J. Am. Chem. Soc.* ***102***, 939-947. https://doi.org/10.1021/ja00523a008.

[12] Barca, G. M. J.; Bertoni, C.; Carrington, L.; Datta, D.; De Silva, N.; Deustua, J. E.; Fedorov, D. G.; Gour, J. R.; Gunina, A. O.; Guidez, E.; Harville, T.; Irle, S.; Ivanic, J.; Kowalski, K.; Leang, S. S.; Li, H.; Li, W.; Lutz, J. J.; Magoulas, I.; Mato, J.; Mironov, V.; Nakata, H.; Pham, B. Q.; Piecuch, P.; Poole, D.; Pruitt, S. R.; Rendell, A. P.; Roskop, L. B.; Ruedenberg, K.; Sattasathuchana, T.; Schmidt, M. W.; Shen, J.; Slipchenko, L.; Sosonkina, M.; Sundriyal, V.; Tiwari, A.; Vallejo, J. L. G.; Westheimer, B.; Wloch, M.; Xu, P.; Zahariev, F.; Gordon, M. S. (2020). Recent developments in the general atomic and molecular electronic structure system. *J. Chem. Phys.* ***152***, 154102. https://doi.org/10.1063/5.0005188

[13] Bode, B. M. and Gordon, M. S. (1999). MacMolPlt: a graphical user interface for GAMESS *J. Mol. Graphics and Modeling*, ***16***, 133-138. https://doi.org/10.1016/s1093-3263(99)00002-9

[14] Avogadro: an open-source molecular builder and visualization tool. Version 1.2.0n http://avogadro.cc/

[15] Hanwell, M. D.; Curtis, D. E.; Lonie, D. C.; Vandermeersch, T.; Zurek, E.; Hutchison, G. R. (20 12). "Avogadro: An advanced semantic chemical editor, visualization, and analysis platform" *J. Cheminformatics*, *4*:17.

[16] Stepanova, V. A.; Guerrero, A.; Schull, C.; Christensen, J.; Cook, J.; Wolmutt, K.; Blochwitz, J.; Ismail, A.; West, J.; Wheaton, A. M.; Guzei, I. A.; Yu, B.; Kubatov, A. Hybrid synthetic and computational study of solvent-free versatile approach to curcuminoids. Submitted to *J. Org. Chem.* on July 4, **2021** and is currently under review.